Geomorphology 358 (2020) 107117

Contents lists available at ScienceDirect

Geomorphology

journal homepage: www.elsevier.com/locate/geomorph

Hydro-morphometric parameters controlling travel distance of pebbles and cobbles in three gravel bed streams

Louis Gilet [a,*], Frédéric Gob [a], Emmanuèle Gautier [a], Geoffrey Houbrechts [b], Clément Virmoux [a], Nathalie Thommeret [c]

[a] Université Panthéon-Sorbonne (Paris 1), Laboratoire de Géographie Physique, CNRS UMR8591, 1 Place Aristide Briand, FR 92195 Meudon cedex, France
[b] University of Liège, Department of Geography, Hydrography and Fluvial Geomorphology Research Centre, B-4000 Sart-Tilman, Belgium
[c] Laboratoire Geomatique et Foncier, CNAM-ESGT, 1 Boulevard Pythagore, 72000 Le Mans, France

ARTICLE INFO

Article history:
Received 18 April 2019
Received in revised form 21 February 2020
Accepted 22 February 2020
Available online 24 February 2020

Keywords:
Bedload travel distance
Stream impulse
Relative grain size
Bed slope
Gravel-bed rivers
PIT tags

ABSTRACT

This study investigates the parameters controlling bedload distances in several gravel-bed rivers of a medium mountain (Morvan, France). Using PIT tags introduced into pebbles and cobbles, an examination of the relationship between several hydro-morphometric variables and travel distance was first undertaken with bivariate analysis. Bedload distances of our 6 study sites show important differences and this discrepancy cannot fully be understood considering only the stream power for the peak discharge, especially in multi-peak surveys such as ours. Stream impulse, a variable combining flow intensity and flow competence duration, has a stronger correlation with bedload distances. The analysis also indicates a varying influence of relative grain size, relative flow depth, bed slope and width/depth ratio. Among all these parameters, in order of importance, the relative grain size, the slope, and the stream impulse, emerge as the most significant explanatory variables from a multivariate analysis. The role of the relative grain size on bedload transport underlines the importance of grain size sorting and microtopography in plane-bed rivers. The influence of the slope is ambivalent: favoring bedload distances under certain circumstances and lowering them under others. The direction of the influence of the slope seems to depend on its combination with other morpho-sedimentary or hydraulical parameters. Finally, we propose a single equation for bedload distance prediction that predicts travel distance rather well.

1. Introduction

Bedload travel distance and derived bedload velocity are key features of sediment transport and channel form dynamics. Indeed, bedload velocity controls the rhythm of bar migration (Jaeggi, 1987), pool-bar sequences (Pyrce and Ashmore, 2003a, 2003b), sediment wave propagation (Madej and Ozaki, 1996; Sutherland et al., 2002) and gravel dispersion (Haschenburger, 2011). Bedload distance and velocity are also used for the calculation of bedload discharge (Laronne et al., 1992; Haschenburger and Church, 1998; Liébault and Laronne, 2008; Houbrechts et al., 2012, 2015; Dell'Agnese et al., 2015; Mao et al., 2017a). However, among the very large amount of papers that discuss bedload transport, few focus on travel distance and a lot remains to be done to truly understand the parameters that influence bedload distances and transport velocity.

Particle size is of course a fundamental component to consider when studying sediment transport, for entrainment conditions as well as for displacement length (Robert, 2003). Most of the studies using tracing techniques show that smaller particles tend to cover larger displacements than coarser fractions of the tracers (Hassan et al., 1991; Church and Hassan, 1992. Lenzi, 2004; Scheingross et al., 2013; Schneider et al., 2014). Ferguson and Wathen (1998) emphasized, however, that the influence of the grain size on travel distances (inverse correlation) was more significant for the coarsest fractions of the riverbed substrate. Wilcock (1997) and Lenzi (2004) observed in their studies that displacement length was dependent on the particle size only for coarser sediment moving under partial transport conditions. It was independent of the grain size for smaller, fully mobile grain size fractions. On their side, Church and Hassan (1992) found that the inverse correlation between travel distance and particle size was less obvious for smaller grain-size fractions because they were more frequently and more efficiently trapped within substrate arrangements (buried, locked or constrained within an imbricated structure).

When reviewing the literature, it also appears that the time scale is key when analyzing the relationship between travel distance and grain size. Phillips and Jerolmack (2014) observe a solid inverse correlation between distance and grain size for cumulated displacement length after many hydrological events, whereas the same inverse correlation is weak for the individual flood scale. A poor correlation between grain

* Corresponding author.
E-mail address: Louis.GILET@lgp.cnrs.fr (L. Gilet).

https://doi.org/10.1016/j.geomorph.2020.107117
0169-555X/

size and virtual velocity of tagged particles is also observed by Mao et al. (2017b) on a short time scale study. Beyond the grain size factor, bedload propagation rates tend to slow down with time (Ferguson et al., 2002), with vertical mixing and progressive burial of the gravel greatly contributing to its slowdown. This is obviously strongly connected to the magnitude and frequency of flood events (Houbrechts et al., 2015). But storage of gravel in less active and lower energy zones such as point bars, plunge pools and logjams may also moderate the particle displacement (Pyrce and Ashmore, 2005; Houbrechts et al., 2015).

Some studies evaluate the relationship between bedload displacement length and hydrological, hydraulic and morphological parameters that are known to affect or reflect rivers' energy, flow resistance and/or particle resistance to entrainment (Church and Hassan, 1992; Hassan and Church, 1992; Lenzi, 2004; Liébault and Clément, 2007; Lamarre and Roy, 2008; Milan, 2013; Phillips and Jerolmack, 2014; Houbrechts et al., 2015; Papangelakis and Hassan, 2016; Klösch and Habersack, 2018). Most of these authors analyze their displacement results in relation to the excess energy above threshold conditions (number of mobilizing floods, competent flow duration, discharge, velocity, specific stream power, shear stress, etc.) but such a relationship is still not yet clearly established (Hassan and Bradley, 2017).

This study explores the hydrological and morphological parameters that control the bedload travel distances in three French gravel-bed rivers. In the medium-sized Morvan mountain (central France), our research investigates the role of relative grain size, bed slope, relative flow depth, width/depth ratio, energy magnitude and flow duration on travel distance on plane-bed rivers. To do so, bedload transport was studied on six study sites among three different rivers, all located in the same regional morpho-climatic context. The influence of specific hydro-morphometric characteristics on bedload transport processes at a-site scale is explored. For every site, we undertook a two-steps analysis: (i) simple bivariate analysis in order to test the influence of the control parameters on the bedload distance; followed by (ii) a multivariate analysis allowing a single relationship for travel distance prediction to be proposed for all of our studied rivers.

2. Study sites

The Morvan massif is a hercynian medium mountain located in the southeast of the Seine catchment (central France) where maximum relief elevation reaches 902 m. (Fig. 1A–B). Its substratum is mainly granitic and gneissic rocks and its climate is temperate oceanic with pluviometry influenced by the orography. The mean annual precipitation in the region is about 900 mm. Combined with the imperviousness of the substratum, this has led to the formation of a channel network featuring a high drainage density.

Six river reaches of three gravel-bed rivers of this region were studied: three on the Yonne river (between 388 and 343 m elevation and, 71 and 83 km^2 for the drainage area), two on the Cure river (between 445 and 295 m elevation, and 160.5 and 234 km^2) and one on the Chalaux river (approximately 395 m elevation, and 69 km^2) (Fig. 1B). They may be considered as medium energy streams with specific stream power for the bankfull discharge fluctuating between 45 and 167 W/m^2 for slopes ranging from 0.0056 m/m to 0.015 m/m (Table 1). The order of the grain size distribution of the bed corresponds rather well to that of the slope values (Table 1). The bed D_{50} and D_{84} range respectively between 0.074 and 0.265 m and 0.105 and 0.699 m, indicating riverbeds dominated by cobbles or small boulders (Table 1 and Fig. 2). With the exception of site S3, our study sites are rather homogeneous and present morphologies that could be qualified as plane-bed. On S3, the grain size distribution is wider and the bed morphology tends to resemble either a light step-pool system or a transverse ribs system (Fig. 2B). Finally, it should be pointed out that the hydrological regimes of some of our study sites are note quite natural as the hydrological regimes are regulated by the releases of a large dam upstream of the Cure river (Settons dam, built in 1858) and by two smaller ones on the Yonne River (Pierre Glissotte and Moulin Blondelot dams, built in the mid-1920s) (Fig. 1B).

The Settons dam was built in 1858 in order to float wood logs. It allowed artificial floods to increase the river's capacity to transport logs that were injected from the river banks at the same time. It is 19 m high and 267 m wide and has a reservoir of 22.7 Mm^3. It is located about 17 km and 31 km respectively upstream of the S3 and S2 study sites. Nowadays, its only function consists of enabling the practice of nautical sports about 30 days/year thanks to water releases. These water releases are mainly operated in spring and autumn, in order to reach a 5 m^3/s discharge on average, and 7/8 m^3/s very occasionally. Those values correspond to 30 to 50% of the bankfull discharge at the downstream study sites. Also, the Settons dam does not control peak flow significantly, as shown on Fig. 3B. This is why the study sites located downstream (S2 and S3) have been considered as non-influenced in the rest of this paper. This assessment is also true for S8, which was not influenced hydrologically by the Pierre Glissotte dam (Fig. 1B) because its reservoir was entirely full of sediment preventing any discharge control (Gilet et al., 2018). S8, located 1.3 km downstream, presents therefore the same hydrological regime as the upstream non-influenced site (S6, Fig. 3C). S7 is the only site that should be considered as moderately influenced because it is located in a by-passed reach, 300 m downstream of the Moulin Blondelot dam (Fig. 1B). The maximum by-passed discharge is 2.3 m^3/s (for a bankfull discharge of 5.5 m^3/s), but large floods mainly flow through the by-passed reach as they remain poorly affected by the small size of the reservoir (700 m^3) (Fig. 3D). Finally S5 (Fig. 3A) and S6 (Fig. 3C) are located upstream of the dams (Fig. 1B) and they are thus not hydrologically influenced.

3. Methods

3.1. Hydrological monitoring

Two public hydrometric stations provide instantaneous discharges: one located on the Yonne river, 3.3 km downstream of the Pierre Glissotte dam and the other on the Cure river, 28 km downstream of the Settons dam (Fig. 1B). In addition, water sensors (Diver, ©Schlumberger) were installed at the upstream and downstream limits of the 6 study sites. They recorded water level variations every 15 min. Coupled with a DEM built from topographical surveys (Section 3.2), the upstream and downstream water altitude enabled the reach averaged water depth to be calculated for a given discharge using the HEC-RAS software.

Water levels from water sensors were transformed into discharges with stage-discharge relationships built from our own discharge measurements (electro-magnetic current-meter) and extrapolation from the two public hydrometric stations (using the catchment area-discharge relationship found in Bravard and Petit, 1997). Even though extrapolation always brings uncertainties, comparisons with reference values (extrapolated discharges and our own discharge measurements) gives us a high level of confidence in our stage-discharge relationships (between 25 and 28 compared values per site; *P*-value min: 2.2e-16 <, P-value max: 4.8e-14; $0.93 \leq R^2 \leq 0.99$). The "energy" of the flow was assessed through the calculation of several parameters. Firstly, the specific stream power of the maximum peak discharge that occurred between two surveys of marked particles was calculated. The specific stream power was calculated using Bagnold's (1980) equation:

$$\omega = \rho g Q S / w \quad (1)$$

with ρ the density of water (kg/m^3); g the acceleration due to gravity (m/s^2), Q the discharge (m^3/s), S the slope (m/m) and w the width of the water-surface (m).

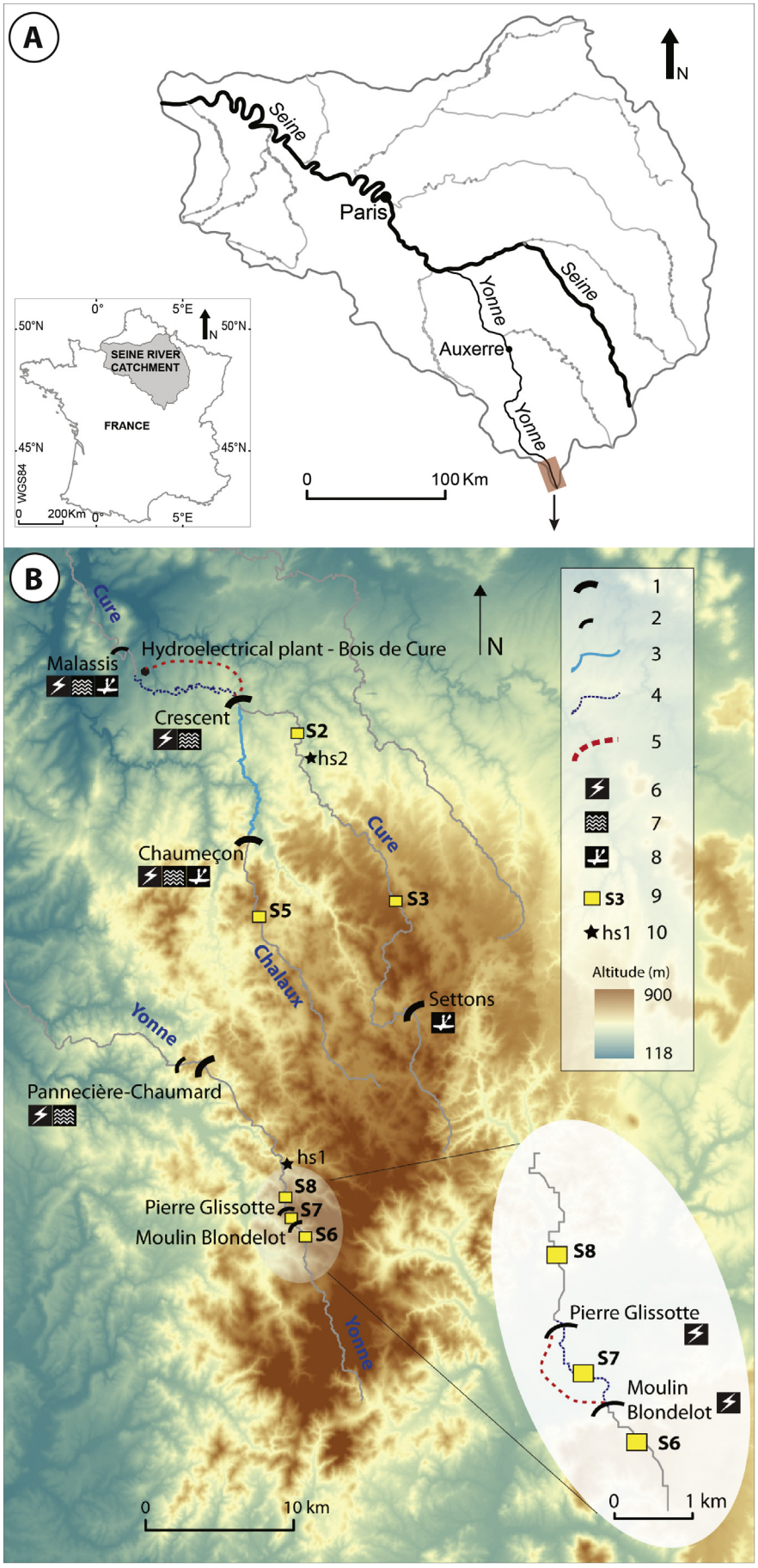
A
N
Seine
Paris
Seine
Yonne
Auxerre
Yonne
0
100 Km
0°
5°E
50°N
45°N
SEINE RIVER CATCHMENT
FRANCE
WGS84
0
200Km
B
N
Cure
Hydroelectrical plant - Bois de Cure
Malassis
Crescent
S2
hs2
Cure
Chaumeçon
S5
S3
Chalaux
Settons
Yonne
Pannecière-Chaumard
hs1
S8
Pierre Glissotte
S7
Moulin Blondelot
S6
Yonne
0
10 km
1
2
3
4
5
6
7
8
S3 9
hs1 10
Altitude (m)
900
118
S8
Pierre Glissotte
S7
Moulin Blondelot
S6
0
1 km

Table 1
Characteristics of the study sites.

Site number and river	S2 Cure	S3 Cure	S5 Chalaux	S6 Yonne	S7 Yonne	S8 Yonne
Catchment area (km^2)	234	160.5	69	71	74,5	83
Mean annual discharge (m^3/s)	4.76	3.51	1.65	1.84	1.93[a]	2.15
Bankfull discharge (m^3/s)	20.5	16	6.2	6	5.5	9.5
Specific stream power for bankfull discharge (W/m^2)	78	166.7	48	45.2	77.1	67.7
Bankfull width (m)	18.05	14.12	7.1	9.5	10.5	11.7
Bed slope (m/m)	0.007	0.015	0.0056	0.0073	0.015	0.0085
D_{50} (m)	0.133	0.265	0.080	0.074	0.108	0.083
D_{84} (m)	0.224	0.699	0.142	0.105	0.247	0.175
D_{16} (m)	0.051	0.041	0.023	0.034	0.038	0.037
D_{84}/D_{16} (sorting index)	4.41	17.17	6.17	3.09	6.50	4.69

[a] Reconstructed natural flow, if there was not a diversion of the discharge from the upstream Moulin Blondelot dam.

In order to consider the entire amount of energy exerted on the bed, the stream power and duration of the peak flows of secondary flood events may also be considered. To do so, integration of flow competence duration was undertaken in diverse contexts over the last thirty years in order to analyze bedload transport and virtual velocity (Hassan et al., 1992; Gintz et al., 1996; Ferguson and Wathen, 1998; Ferguson et al., 2002; Milan, 2013; Phillips and Jerolmack, 2014; Schneider et al., 2014; Houbrechts et al., 2015; Arnaud et al., 2017; Klösch and Habersack, 2018). In this study we proposed a variant of the dimensionless impulse (I_*) introduced by Phillips et al. (2013) and Phillips and Jerolmack (2014), and expressed as:

$$I_* = \int_{ts}^{tf} \frac{(U_* - U_*c)\, dt}{D50}, U_* > Uc \quad (2)$$

with U_* the shear velocity and U_{*c} the threshold shear velocity for sediment motion, D_{50} the median grain size of the tracers, *ts* and *tf* the starting and finishing times of the considered period. According to Eq. (2), the excess of shear velocity is considered during the delimited period during which sediment transport occurs. These excess values are multiplied by the duration (dt) they are supposed to last and normalized by the D_{50} of the tracers mobilized. In this way, the intensity and duration of the mobilizing flow as well as the particle size is taken into account to examine the river energy consumed for particle transportation. In this study, uncertainties with regard to the calculation of velocities led us to prefer considering specific stream power instead of shear velocity. Consequently, we use an overall time-integrated excess stream power called "stream impulse" (SI expressed in Ws/m^3). It can be written as:

$$SI = \int_{ts}^{tf} \frac{(\omega - \omega c)\, dt}{D50}, \omega > \omega c \quad (3)$$

with ω as described in Eq. (1). In this form SI is rather similar to the excess flow energy expenditure calculated by Haschenburger (2013) and Schneider et al. (2014) that reflects the same idea of calculating a time-integrated excess stream power (Hassan and Bradley, 2017). Mao et al. (2017b) also show the importance of considering the whole flow series in order to underline the influence of high antecedent flows on incipient motion of sediments and on their virtual velocity.

The slope and width needed for the calculation of stream power are both known from topographical surveys: the former corresponds to the reach averaged bed slope and the latter to the reach averaged bankfull width. Critical stream power is calculated from the critical discharge. This is a key parameter as it conditions the whole calculation of excess energy consumed for particle displacement. Incipient motion may be approached empirically using PIT tags and a mobile antenna, but this requires multiple surveys after single low to moderate peak flows. Considering the aims of this study, we have chosen to focus instead on longer time series that include several moderate and high peak flows. Consequently, the lowest mobilizing peak discharge (Q_{lmp}) we may use to determine critical conditions remains for some study sites rather high and the distances covered by the tracers after this peak are relatively long. When compared to the bankfull discharge (Q_{bf}), Q_{lmp} fluctuates between 0.83*Q_{bf} and 1.15 Q_{bf} on our 6 study sites for a wide grain size of tagged particles including the large ones (following the study sites, between D_2 and D_6 of the tracers' distribution for the finest mobilized grains, to D_{86} and D_{96} for the coarsest ones). The literature shows that these values are very likely excessive and rather indicates that critical discharges range between 0.25 and 0.8 Q_{bf} (Andrews and Nankervis, 1995; Bravard and Petit, 1997; Moog and Whiting, 1998; Pitlick and Cress, 2000; Assani and Petit, 2004; Houbrechts et al., 2006, 2015; Papangelakis, 2013; Phillips, 2015). Only Métivier et al. (2017) and Pfeiffer et al. (2017) found incipient motion close to bankfull conditions. Pfeiffer et al. (2017) demonstrated still that τ_{*c} was about 2.35 times lower in the West coast rivers (USA) because of surface armoring. Petit et al. (2005) gave several examples of bedload mobilization around 0.7 Q_{bf} in gravel bed streams similar in size, slope and substrate to those of the Morvan. Accordingly, we chose to consider a unique theoretical critical discharge of 0.7 Q_{bf}. This choice was also guided by a few direct additional observations made during gauging campaigns of several of our sites indicating that the bed material began to move for discharges ranging from 0.5 to 0.7 Q_{bf}. Although the critical discharge may not equate exactly to 0.7 Q_{bf} for all of our sites, this approach enables a consistency of the error between the sites.

3.2. Morphological data and grain size distribution

Longitudinal profiles and the cross sectional geometry of the study sites were surveyed with a Trimble total station S6. At least 13 cross sections spaced by 1.5 times the bankfull width were made on each site. These topographical surveys were then used to calculate the bed slope and build a DEM on GIS (Arcgis software), which was then loaded into HEC-RAS software (Section 3.1). The grain size distribution of the riverbed was determined using Wolman's surface sampling method (Wolman, 1954). We tried to respect a sampling step equating to twice the b-axis of the largest particle of the sampled unit (Lejot, 2008; Belliard et al., 2009). Three sub-reaches were delimited along the study reach as a function of their apparent geomorphological homogeneity (bankfull width and depth, grain size range, substrate arrangement) even if geomorphological variations within the same reach were generally very limited. At least 100 particles per sub-reach were sampled and measured, resulting in a minimum of 300 particles per site.

3.3. Bedload transport monitoring

Bedload transport was studied with Radio Frequency Identification (RFID) technology. Individual particles were tagged with a Passive

Fig. 1. Locations maps: A) The Morvan massif in the Seine river catchment, B) The study sites on the Yonne and Cure rivers. 1. Large dams (>15 m); 2. Medium size dams (<10 m); 3. Regular water-releases; 4. By-passed reach; 5. By-passed canal; Dam function: 6. Hydroelectricity; 7. Flood control; 8. Nautical sports; 9. Study site; 10. Hydrometric station.

Fig. 2. Photographs of the study sites during low or medium flows.

Integrated Transponder (PIT) that can be identified by a unique number thanks to the RFID technology. This is now commonly used for bedload transport studies (Lamarre et al., 2005; Rollet et al., 2008; Liébault et al., 2012; Bradley and Tucker, 2012; Chapuis et al., 2014; Phillips and Jerolmack, 2014; Houbrechts et al., 2015; Dépret et al., 2017). The technique presents numerous advantages and a series of limits well described by Piégay et al. (2016). Among the benefits of the technique, are the fact that the tracers are not disturbed between detections, as well as the relatively low cost and the long lifetime of the tag. With regard to limitations, one may mention that this is a time consuming method, there is an initial modification of the bed structure when sampling the bed, and the PIT tags cannot be detected when buried under a range of sediment depth values varying between 20 cm (Houbrechts et al., 2012), 45 cm (Chapuis et al., 2014) and 70–89 cm (Arnaud et al., 2015), for the "small" circular antennas that we used. During our field surveys, in the few instances when it was possible to test this detection range, it appeared that tracers were hard to detect beyond 25 cm of burial depth.

In this study, 50 tagged particles (tracers) were first injected at each site between August and October 2014 (Table 2). At the study sites with active bedload transport, some initial tracers may rapidly have been able to go farther than the prospected area. 25 additional tracers were then injected in October 2015. The particles to tag were selected in the riverbed using the Wolman coarse grain sampling method (1954). However, the tracers' size range does not completely follow grain size distribution of the bed because the tags we used were 32 or 23 mm long. Consequently, no particle with a b-axis under 20 mm was tagged. Also, for logistical reasons we were not able to tag more than few particles per site with a b-axis above 130 mm. This led to a slight discrepancy between the D_{50} injected and the D_{50} of the bed, that is accentuated with the D_{84} percentile (Table 2). On sites with the largest grain size, this could have led to a slight overestimation of the mean distance travelled by the tracers over the potential mean distance travelled by the "unmonitored" bedload. This possible overestimation of the travel distance is discussed in Section 5.5.

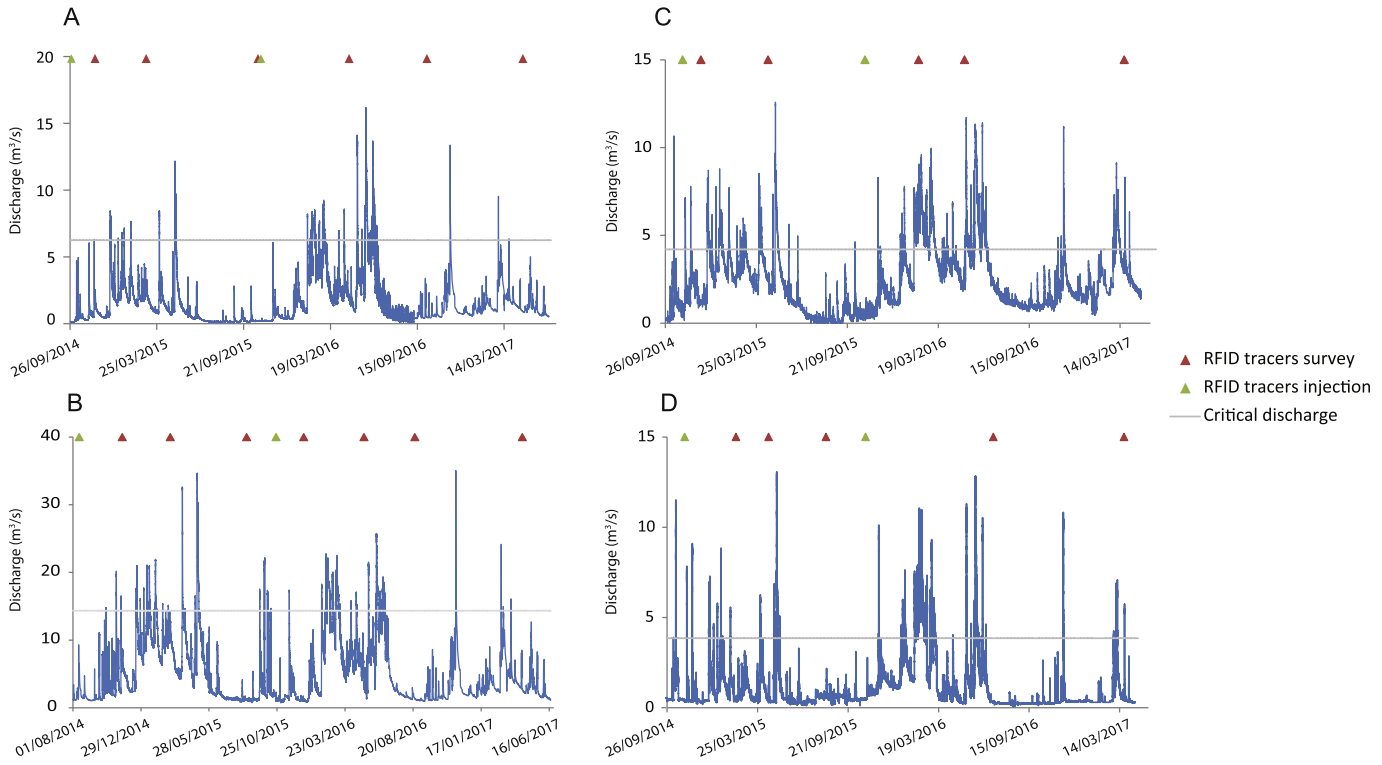

Fig. 3. Discharge recorded on S5 Chalaux (A), S2 Cure (B), S6 (C) and S7 (D) Yonne sites. The vertical and horizontal axes do not have the same scales on the four graphs and the study period on S2 begins earlier. The hydrological regime of S2 is the same as S3, located about 14 km upstream and the hydrological regime of S6 is the same as S8, located about 6 km downstream. The method for the estimation of the critical discharge (for sediment entrainment) is detailed in Section 3.1.

Tracers were injected along the cross sections at an interval of 1.25 m. Each cross section was separated by at least 2 m. Surveys of the tracers' positions were undertaken between November 2014 and April 2017 with a round, 0.55 m-diameter antenna. The distances travelled by the marked particles were measured using a flexible ruler (tape measure) unrolled along the bank. Due to the degree of precision of the measurements (antenna radius: 0.5 m), tracers were considered as mobile when they had moved forward at least 0.6 m beyond their previous known position for the first 80 m of the study sites. Beyond 80 m, we considered mobilization if the tracers moved >1 m. This increase in error margin is based on the observation that beyond a 75–85 m length, noticeable disparities (from 0.02 m to 0.06 m) in the ruler roll-out between two surveys can appear owing to irregularities along the bank (trees, boulders).

Except if mentioned otherwise, the displacements recorded during the first survey after injection are not displayed in the results below. Even if tracers were carefully inserted within the alluvial substrate, by excluding the displacements recorded during the first survey we aim to prevent any “artificial” protrusion effect favoring tracers' mobility (Bright, 2014; Houbrechts et al., 2015; Olinde and Johnson, 2015).

In addition, we paid attention to only compare the monitoring results of tracers obtained with equally good surveying flow conditions: i.e. when the water level and flow strength were low enough to prospect >90% of the reach area (except for the specific S6 site, where a section of the fluvial reach between 120 and 160 m length is permanently hard to access because of water depth and slippery substrate). In the end, except when cumulative distances are discussed in Section 4.1, the bedload data presented in this paper come from three surveys realized on each of the Yonne sites (S6, S7, S8), four surveys on the Chalaux (S5) and S3 Cure sites, and five surveys on the S2 Cure site.

4. Results

4.1. Relationship between bedload distances and river energy

Fig. 4 and Table 3 give a first overview of the cumulative bedload transport observed at each site about 2.5 years after the injection of the first tracers. One may first notice a different intensity according to the rivers: the Yonne and the Chalaux appear to be rather dynamic systems (in terms of distance travelled and mobilization rates), while the Cure presents lower bedload transport activity. A distinction may however be made between the S2 Cure site and the S3 Cure site. S2 presents medium transport activity but a mean travel distance close to the S6 Yonne site, while the S3 site shows a noticeably low transport activity. At all of the study sites considered, the mean distance travelled by the tracers varies between 24 m to 315 m over about 2.5 years (the

Table 2
Details of the injected PIT tag tracers.

Site and river	S2-Cure	S3-Cure	S5-Chalaux	S6-Yonne	S7-Yonne	S8-Yonne
Injection date (50 first tracers)	15/08/14	16/08/14	29/09/14	30/10/14	31/10/14	31/10/14
Last survey date (duration in years)	18/04/17 (2.7)	20/04/17 (2.7)	22/04/17 (2.6)	22/03/17 (2.4)	24/03/17 (2.4)	23/04/17 (2.5)
Total number of tracers	75	50	75	75	75	75
D_{50} injected tracers (mm)	63	60	62	58	58	63.5
D_{50} injected tracers / D_{50} riverbed	0.47	0.23	0.78	0.78	0.55	0.76
D_{16} injected tracers / D_{16} riverbed	0.88	0.97	1.86	0.97	1.02	1.13
D_{84} injected tracers / D_{84} riverbed	0.50	0.13	0.68	0.79	0.37	0.55

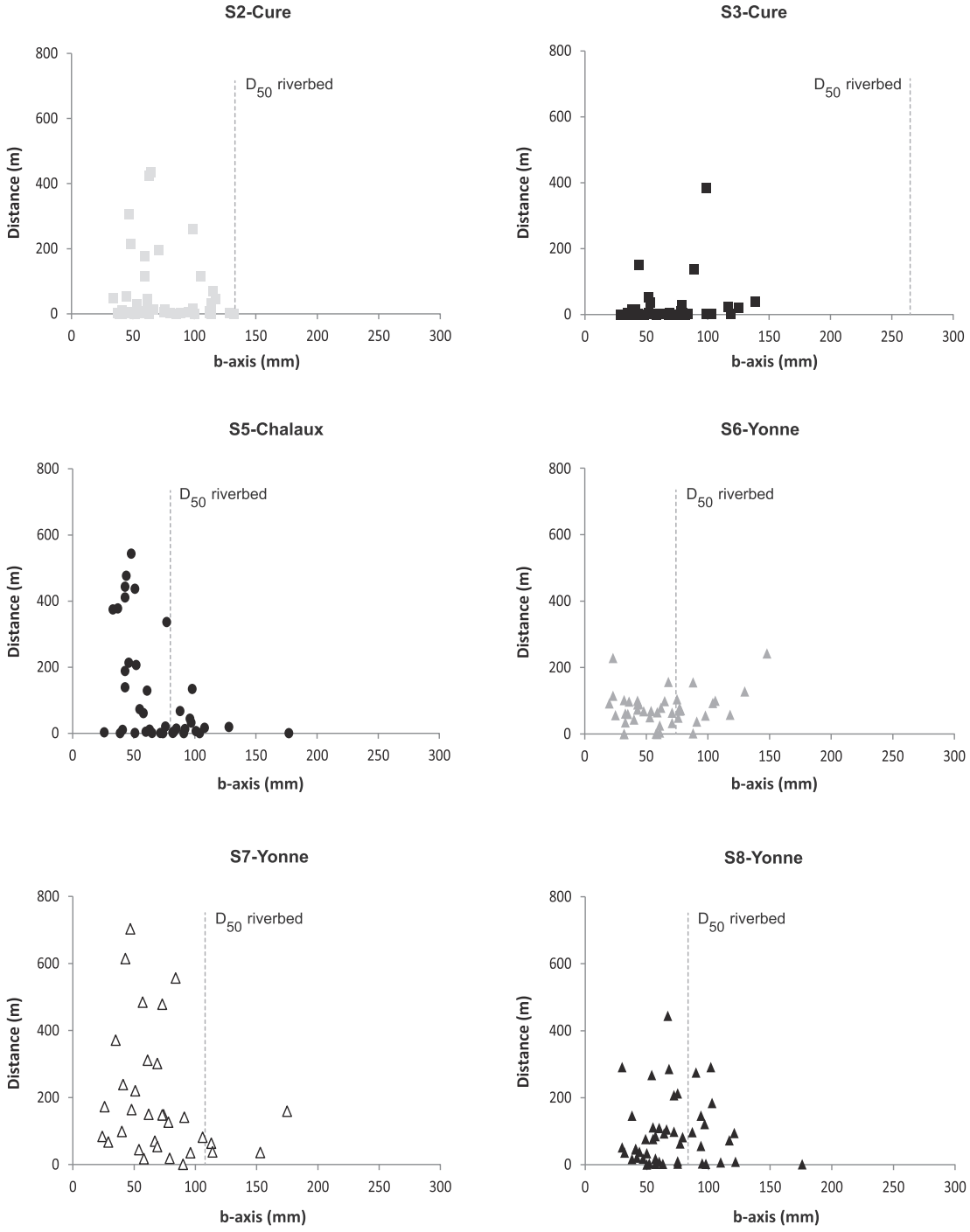

Fig. 4. Relationship between cumulative bedload distances and the median diameter of tracers. Distances are based on the results of the last monitoring survey only.

Table 3
Cumulative data on bedload transport in Morvan rivers.

Site and river	S2-Cure	S3-Cure	S5-Chalaux	S6-Yonne	S7-Yonne	S8-Yonne
Mean distance (m)	67.5	24	141	78	315	123
Di_{max} mobilized (mm)	144	139	128	148	175	122
D_{50} tracers (mm)	62.5	59	73	69.5	61	75
D_{50} mobilized tracers (mm)	63	65.5	58	61	58	68
Mobilization rate	0.69	0.50	0.80	0.91	0.97	0.94

Distance values are based on the results of the last monitoring survey only and the mean values include tracers that did not move. The D_{50} tracers represents the median grain size of the detected tracers, including tracers that did not move. D_{50} mobilized tracers includes only mobile tracers.

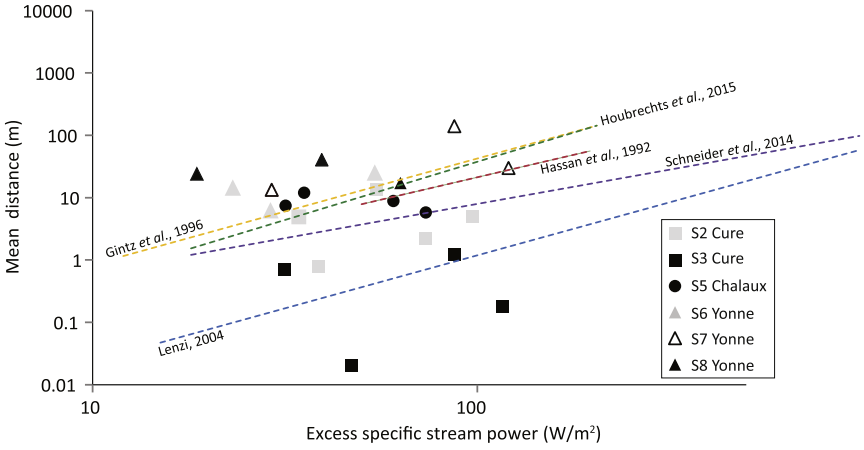

Fig. 5. Relationship between the mean inter-survey distance (0 values included) and the maximal inter-survey excess specific stream power.

cumulative travel distances at S6 are probably underestimated as mobile tracers located in the previously mentioned "hard to survey" subreach, between 120 and 160 m, are not taken into account). If we exclude S6, the largest particles injected have not been significantly transported (or not transported at all) and sediment sorting has clearly developed on sites S2, S5, S7 and, in a less obvious way, on S8. In Table 3, the D_{50} of the mobilized tracers is close to or slightly under the median size of all detected tracers (i.e. D_{50} tracers, which does not exactly equate to the injected tracers' D_{50} from Table 2) and is therefore still much smaller than the D_{50} of the bed (Table 1).

4.1.1. Excess stream power and duration of the competent flow

The excess stream power of the highest peak discharge between two PIT tag surveys is compared in Fig. 5 to the mean distances travelled during this same period. Though the data set of our 6 study sites is rather coherent with observations from the literature (Hassan et al., 1992; Gintz et al., 1996; Lenzi, 2004; Schneider et al., 2014; Houbrechts et al., 2015), no evident relationships appear and the data presents a large scatter around the literature relationships. This large dispersion of the data first reflects a certain diversity of functioning between the different sites despite the apparent homogeneity of the rivers studied. This suggests that the inner diversity of the sites (slope, channel geometry, roughness and structure of the bed) has to be explored in detail. The Cure river experienced much shorter displacement than the other river reaches. Yet S3 is the study site presenting the steepest slope (0,015 m/m), the largest D_{50} (26.5 cm) and the highest D_{84}/D_{16} ratio (17.17) (Table 1). The potential influence of high bed roughness on the displacement of particles should be investigated further.

Indeed another notable issue appears from the Fig. 5. There is a very poor relationship between excess stream power and the corresponding mean distance (even within the same site). Indeed if a regression line were plotted for each site, most of the time the surveys involving the most powerful peak flows would never correspond to the longest mean distance travelled. The correlation is even negative in many instances, with travel distance relatively shorter for the largest flood events. The magnitude of the highest flow peak is in our case not sufficient to describe travel distance.

4.1.2. Stream impulse

In order to combine duration and magnitude of the overall flow over the critical threshold, we considered the stream impulse (SI) presented in the Eq. (3). Fig. 6 shows the relationship between SI and the corresponding mean distance. It shows that the use of stream impulse is more adapted for the understanding of our bedload distance data.

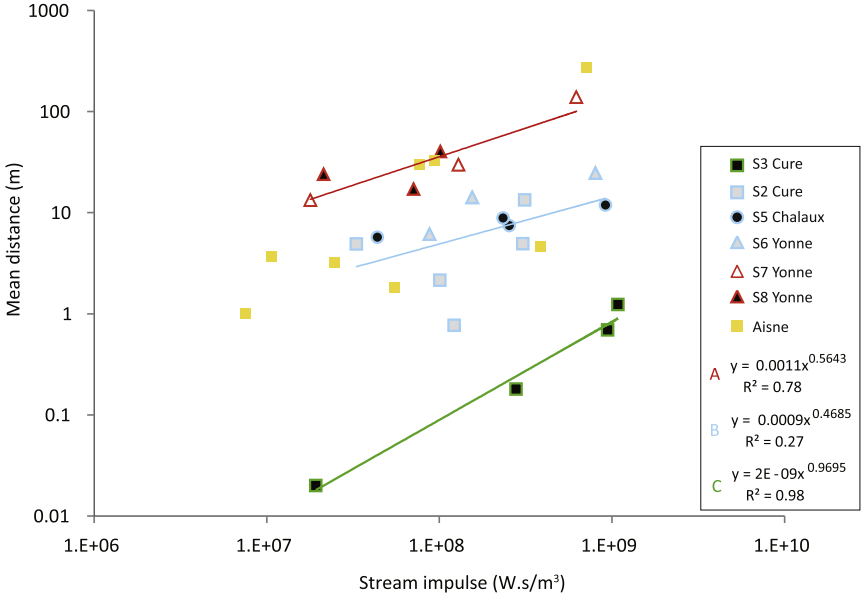

Fig. 6. Relationship between the mean travel distance and the stream impulse (SI). Colored borders of dots and colored curves highlight the three groups (A, B, C) that have been distinguished.

Indeed, almost all sites show a clearer positive relationship between energy, flow duration and travel distance. Three groups of sites appear now rather clearly. They are mainly based on the differences of distance range for a given stream impulse range and they gather sites with some common morphological features.

The first group concerns the most dynamic sites, S7 and S8 on the Yonne river (regression A, $R^2 = 0.78$. *P*-value = 0.018). The second group gathers the observations of S2, S5 and S6 (regression B, $R^2 = 0.27$, P-value = 0.081). The last one confirms what Fig. 5A and B had already shown: despite similar or higher stream impulse values, the tracers at S3 travel shorter distances than at the other sites (regression C, $R^2 = 0.98$; P-value = 0.01). As already mentioned, S3 is the steepest reach (s = 0.015 m/m) with a stream bed that includes a lot of large cobbles (D_{50} = 26.5 cm). Group A is almost as steep (s > 0.008 m/m) but with smaller particles (D_{50} = 8.3 and 10.8 cm). Meanwhile, group B reaches have lower slopes (s < 0.0075 m/m) but show a wider range of median grain size (7.4 < D_{50} < 13.3 cm). This group may be slightly less homogeneous morphologically (e.g. bankfull width, Table 1). On Fig. 6, the dots from group B are also a bit more scattered (S2 especially) and this explains the low coefficient of determination and their statistical non-significance according to P-value calculation.

Data used by Houbrechts et al. (2015) on the Aisne river were plotted in Fig. 6 for comparison. This river flows in Southern Belgium within a morpho-climatic context quite similar to the Morvan massif. The D_{50} of the bed is 9.2 cm, its slope 0.0053 m/m and its bankfull width 13.57 m, and the critical discharge for particle entrainment represents 55% of the bankfull discharge. The correlation between mean distance and stream impulse is also rather obvious for the Aisne data (R^2 = 0.53; P-value = 0.04). The Aisne scatter plot shows a trend similar to the Morvan's A and B relationships.

Despite “time” and “storage processes” as potential complexity factors on the Aisne river (see Discussion Section, 5.2), Fig. 6 shows clearly that using the stream impulse (SI) allows the description of the travel mean distance of the tracers to be greatly improved. Nonetheless, the dispersion of the Morvan data remains quite large and, at this stage, the reasons why still have to be clarified.

4.2. Relationship between bedload distances and morpho-hydraulic parameters

The mean travel distances of tracers have been normalized by different morphological and hydraulic parameters (Fig. 7A–D) in order to

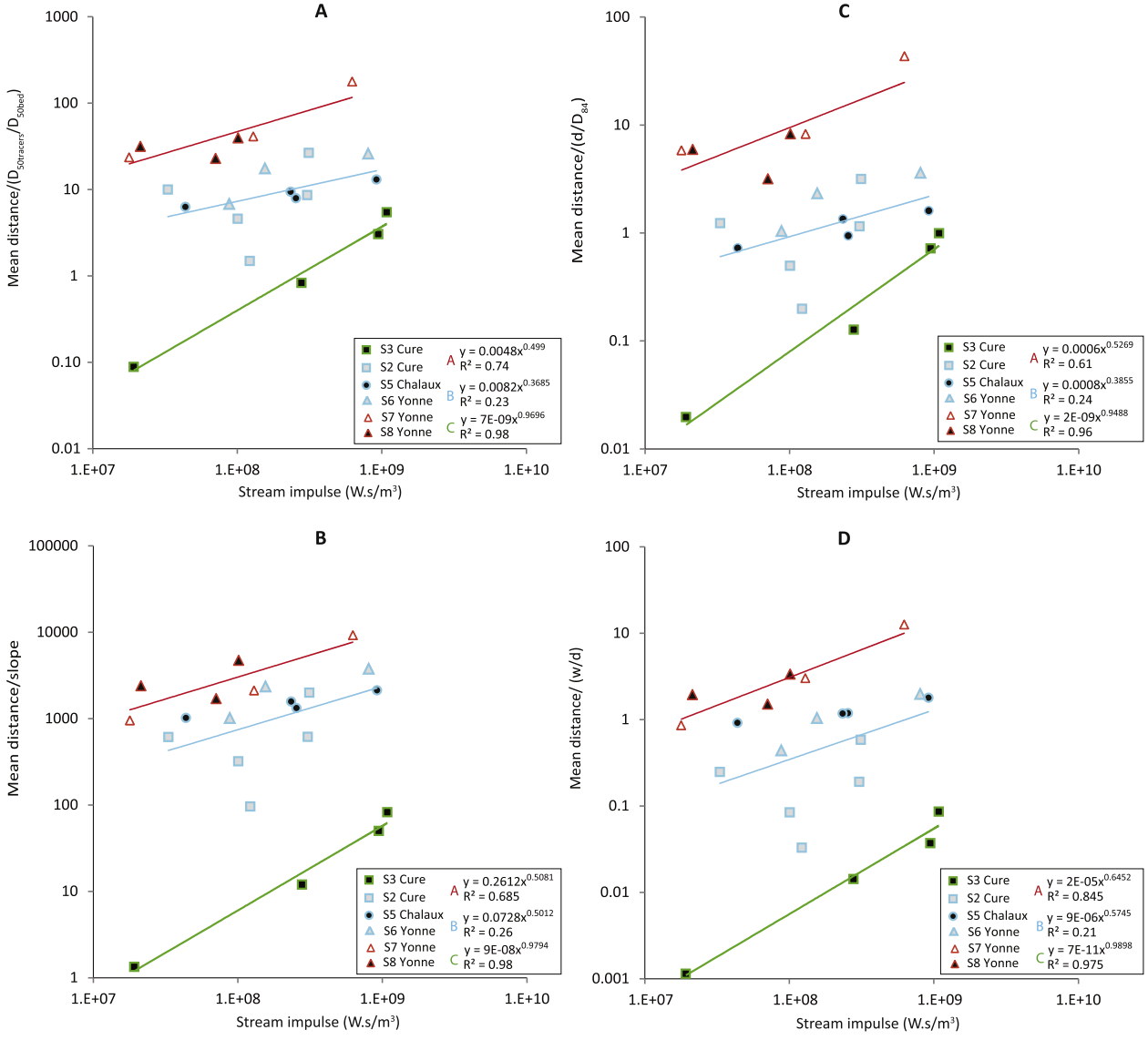

Fig. 7. Relationship between mean travel distance normalized by hydro-morphometric parameters and stream impulse (SI). A) Mean travel distance normalized by relative grain size, B) Mean travel distance normalized by the bed slope, C) Mean travel distance normalized by relative flow depth, D) Mean travel distance normalized by the width/depth ratio. Equations correspond to the best-fit relationship.

Table 4
Mean values of the morpho-hydraulic parameters.

Site and river	S2-Cure	S3-Cure	S5-Chalaux	S6-Yonne	S7-Yonne	S8-Yonne
Mean[a] relative grain size of the tracers	0.51	0.23	0.93	0.88	0.69	0.84
Bed slope (m/m)	0.007	0.015	0.0056	0.0073	0.0015	0.0085
Mean[a] relative flow depth	4.14	1.14	7.43	6.25	3.03	4.76
Mean[a] width/depth ratio	23.5	17.2	6.7	13.3	12.1	11.8

[a] Corresponding to the mean value of the different RFID surveys or inter-survey periods.

identify the reasons behind the discrepancy observed on Fig. 6. The parameters are: relative grain size corresponding to the $D_{50\ tracers}/D_{50\ bed}$ ratio (A), where the first term is the D_{50} of the tracers whose displacement distance is known, immobile tracers included; bed channel slope (B); relative flow depth (C), given by the ratio between the reach averaged water depth for the peak discharge of the inter-survey period and the D_{84} of the bed; and reach averaged width/depth ratio for the peak discharge of the inter-survey period (D).

In Fig. 7A–D, 3 groups of data can be distinguished again and they are globally the same groups described in Fig. 6. However the gap between the relationships fluctuates following the parameter used for normalization, giving a clearer idea of what and how morpho-hydraulic features may influence bedload travel distance on each study site.

The relative grain size is likely to influence S3 travel distances, as can be seen from the normalization in Fig. 7A, which brings S3 closer to the other sites (compared to Fig. 6). The relative grain size of the tracers on this site is by far the lowest (Table 4) and a hiding effect may then contribute to explain the low recorded distances. Compared to Fig. 6, S7 and S8 data are closer to S3 data on Fig. 7A because their tracers have on average a relative grain size that is much higher than the relative size of S3 tracers (Table 4). In S7 and S8, boulders are present but they are less numerous and they are smaller than on S3. S7 and S8's riverbeds are also much better sorted in terms of grain size than S3's riverbed, where a deficit of medium sized particles can be observed (Table 1). The relative grain size may also contribute to the relative scattering of the Group B data for a comparable stream impulse, observed on Fig. 7 as well as on Fig. 6. S5 and S6 present the highest values whereas S2's mean relative grain size is much lower (Table 4).

The different groups of study sites present a more unclear relationship with the bed slope (Fig. 7B). The higher bed slope of the A and C groups ($s \geq 0.008$ m/m, Table 4) increases normalized travel distances to a lesser degree than for the sites of the intermediary group (S2, S5 and S6) which have lower slopes ($s \leq 0.0073$ m/m) (Fig. 7B). S7 and S8 data are then closer to these intermediary sites in Fig. 7B, when S3 appears even more isolated. A significant slope is therefore associated with short (group C) and long (group A) bedload travel distances, and a moderate slope corresponds to the group with intermediary bedload distances (B).

The relative flow depth on S3 group C is also shown as a parameter that may contribute to the low travel distances, as emphasized by its use for normalization that clearly gets S3 data closer to B group (Fig. 7C). The high slope and the presence of boulders on S7 and S8 induces a relative flow depth that is lower than the intermediary B group (except for S2), increasing the disparity between groups A and B (Fig. 7C). Thus, a group of data is showing important bedload displacements despite a low relative flow depth (A) and another shows very short bedload displacements that may be partly explained by a very low relative flow depth (C). In group B, S2 presents a large D_{84} leading to a mean relative flow depth close to S8 and just higher than S7. This is why normalization of mean distances with relative flow depth does not "move" S2 data as far from S7 and S8 as it does for S5 and S6 (Fig. 7C). Indeed, these have the highest relative flow depth values because of lower bed slope, D_{84} and bankfull width values (Table 1 and Table 4). This higher relative flow depth, combined with the higher relative grain size and the substrate homogeneity on S6 (Table 1, index sorting), are hydro-morphometric features that may "compensate" the lower bed slope of these sites. This suggests, however, that (increasing) slope as a parameter fostering bedload transport as on S7 and S8 should be considered. The positive or negative effect of the bed slope will be further questioned in Section 5.4.

In group B, for S5, bedload mean distances may also be supported by a very low w/d ratio, compared to the other sites (Table 4). This may favor increased bedload travel distance as potentially indicating a higher depth during floods and then a higher shear stress for a given discharge. The normalization with this parameter (Fig. 7D) clearly brings S5 data closer to S7 and S8. Inversely, the Cure sites have the highest w/d ratios because of their larger width (S2), or their low flow depth due to bed slope (S3). This maintains S3 normalized distances beneath the other sites' values and lowers S2 data. These even tend to separate from other data of the B intermediary group (Fig. 7D), underlining once again the link between different morpho-hydraulic parameters and scattered bedload distances within this group itself.

4.3. Stepwise multiple linear regression

Simple bivariate regressions of Fig. 7 allowed parameters that discriminate mean travel distance to be identified. However, in order to quantify the degree of influence of each parameter and propose a single relationship allowing mean distance to be predicted, stepwise multiple linear regression was tested. The five parameters tested were chosen according to the results of the bivariate relationships presented above: stream impulse (SI), relative grain size ($D_{50tracers}/D_{50bed}$), relative flow depth (d/D_{84}), bed channel slope (s) and width/depth ratio (w/d). Only three of them were finally defined as having a significant influence during the analysis (Table 5), allowing the following prediction model to be proposed:

$$\overline{L} = \mathrm{EXP}\left(7.3805 + 0.4069\ \mathrm{LN}\,(\mathrm{SI}) + 3,8896\ \mathrm{LN}\left(\frac{D_{50\ tracers}}{D_{50\ bed}}\right) + 2.3694\ \mathrm{LN}\,(\mathrm{S})\right) \quad (4)$$

where $\overline{L}$ is the mean bedload distance, SI the stream impulse, D_{50} tracers is the median grain size of the tracer whose displacement distance is known, immobile tracers included, and S is the bed slope. This model has a quite convincing adjusted coefficient of multiple determination ($R^2 = 0.73$) with a rather good residual standard error of 1.064, *P*-value <0.001 and F-statistic = 17.43.

The model provides quite strong predictions for most of our study sites. Once again it is the S3 site on the Cure that diverges most from the other study sites. In this case, our model poorly predicts two S3 surveys with a clear overestimation of the low tracer displacement (Fig. 8).

Table 5
Results of the stepwise multiple regression.

	Std. Error	t value	P-value r(>|t|)	Significance
Intercept	4.8936	1.508	0.14796	*
Log (SI)	0.1804	2.256	0.03606	*
Log ($D_{50tracers}/D_{50bed}$)	0.5771	6.740	1.93e-06	***
Log (s)	0.8055	2.941	0.00838	**

Codes for significance :
*** = P-value < 0.001
** = P-value < 0.01
* = P-value < 0.05
= P-value < 1

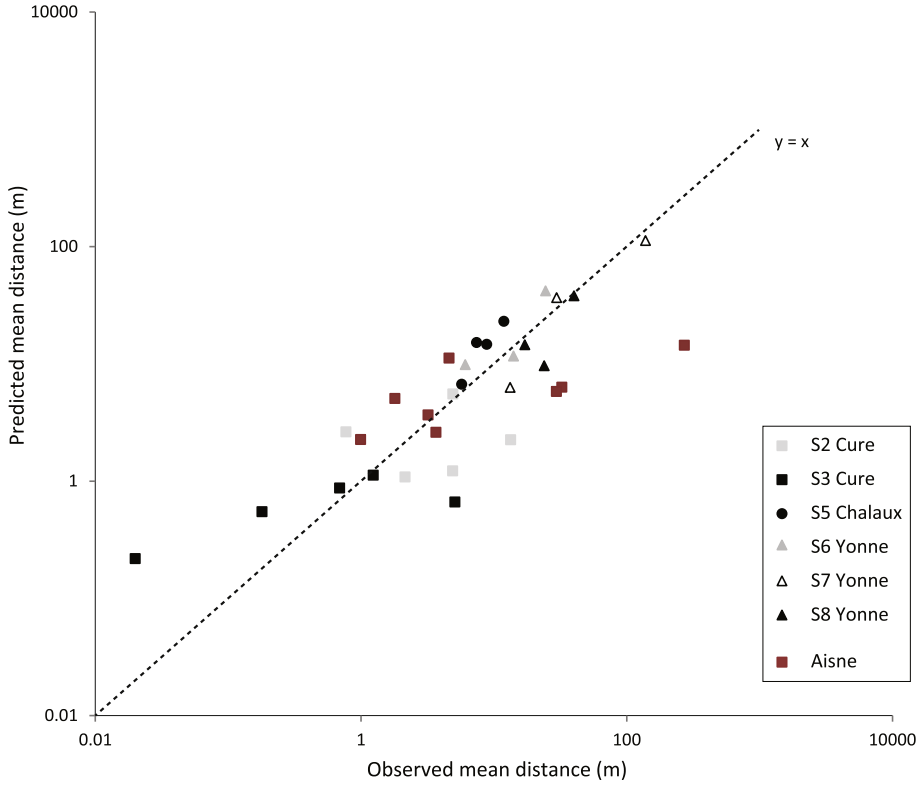

Fig. 8. Comparison between the observed mean distance of tracers and the predicted mean distance from Eq. (4).

A test was also realized with the Aisne river data (Houbrechts et al., 2015). These were not included in the multiple regression analysis that enabled to build the Eq. (4). The test tends to validate the model as we obtain predicted distances that genuinely match for all but one of the observed distances (Fig. 8).

When looking at Fig. 8 in more detail, one may notice a slight offset of certain data towards the bottom of the graph (i.e.) indicating an underestimation of the predicted distance. This concerned notably the three largest mean distances observed on the Aisne river. These three largest mean observed distances on which this underestimation applies were also recorded for three of the four inter-survey periods with the highest stream impulse. A possible underestimation of the stream impulse for high flow events is discussed in the Section 5.2.

5. Discussion

5.1. Bedload dynamics poorly explained by the commonly used hydraulic parameters

Bedload travel distances recorded on Morvan rivers are very different according to the study sites (Table 3 and Fig. 4). Also, for the same site, the travel distance appear moderately correlated with the higher flood peak (Fig. 5A). The longest displacements are rarely coupled with the greatest excess stream power. Conversely, in many instances, the largest events correspond to shorter displacements. This is quite counterintuitive and diverges from what the literature has repeatedly shown (Hassan et al., 1992; Gintz et al., 1996; Lenzi, 2004; Schneider et al., 2014; Houbrechts et al., 2015).

Comparisons with the literature may bring precious information but should be used with caution because of the differences in methodology (first peak or maximal peak discharge considered, tracer replacement, number of flood peaks considered) that may lead to very divergent results. Indeed, Fig. 5 shows that our results do not entirely match with data from the literature. Moreover, while the Morvan data has been acquired only in plane-bed channels, the data from the literature presents a dispersion corresponding to results from a wide range of bed morphologies: fr0om other plane-beds (Houbrechts et al., 2015) to riffle-pools (Hassan et al., 1992; Houbrechts et al., 2015) and even step-pools (Gintz et al., 1996; Lenzi, 2004; Schneider et al., 2014).

The high rate of displacement related to a short inter-survey period observed in our data set for two surveys (S7 and S8) is a good example of this methodological question. They present high distances for a relatively low competent flow duration and low excess stream power peak because of the short period we left between the previous surveys (65 days for S7 and 69 days for S8). Long distance travelled may then have been stimulated by tracers not well inserted in the bed structure and by transport mostly operated during the first hours (or the first event) of the competent flow. These elements echo a recent study from Dell'Agnese et al. (2015) underlining the influence of different flow competent durations on bedload virtual velocity through the capacity to get closer to the actual virtual velocity.

The weak correlation between bedload displacements and the maximal excess stream power of our data may also be explained by the way the excess stream power is calculated (Fig. 5). Indeed, only the highest peak discharges of the inter-survey periods are considered. Meanwhile, each of these periods encompasses several flood peaks of variable magnitude and duration. This, therefore, should lead to noticeable differences with results from "one-peak survey" studies such as those of Gintz et al. (1996) or Houbrechts et al. (2015). With this in mind, considering only the magnitude of the highest peak is clearly not adequate to describe our bedload displacements. The multi-peak characteristics of our surveys forced us to explore the role played by the combination of the magnitude of the high flows and their duration, as suggested by Papangelakis and Hassan (2016) among others.

5.2. Relevance of the stream impulse in a multi-peak survey

Inspired by the dimensionless impulse developed by Phillips and Jerolmack (2014) and echoing the excess energy expenditure used by Haschenburger (2013) and Schneider et al. (2014), the stream impulse

(SI) enables the flow competence duration and the overall excess stream power to be integrated.

On Morvan rivers, the bedload mean distance is clearly better correlated with the stream impulse than with the sole magnitude of the largest peak flow, especially when grouping the data according to the riverbed characteristics (Fig. 7). This should, however, be considered with some nuances as some of these relationships are built on a limited number of dots.

The introduction of independent data from the Aisne river, confirms the relevance of using the stream impulse to characterize the flows. However, the Aisne river data also brings forward the potential influence of time and burial phenomenon (Ferguson and Hoey, 2002; Haschenburger, 2011; Houbrechts et al., 2015). Indeed, the two lowest dots of the Aisne data on Fig. 6 have been surveyed 5.5 and 6.3 years after the initial injection of tracers, when the other monitoring surveys occurred within 3.3 years following the injection, and following a 10-year flood event. This indicates that major events as well as simple elapsed time since injection have probably contributed to vertical mixing and burial of a part of the tracers, making them less easy to entrain and thus reducing the distance travelled. This leads us to emphasize that our study has been realized for a limited duration (about 2.5 years) and to question if the good correlation between travel distance and stream impulse would be maintained on a longer time scale.

The relationship resulting from the stepwise multiple regression (Eq. (4)) also confirms the interest in considering stream impulse to predict the mean distance travelled by the particles. The calculation of the mean distances on the Aisne with this relationship is also rather good except for predictions of distances corresponding to large flow events (Fig. 8). This results in an underestimation of the distance, probably because of the different resolutions in the hydrological data. The Aisne instantaneous discharge data (used to calculate the SI) are indeed measured every hour whereas the Morvan data are measured every 15 min. It is then possible that the highest peak discharges, and consequently the maximum excess stream powers were less precisely recorded for the Aisne river.

5.3. The dominant influence of relative grain size: meanings and trails to explore

Our study supports the idea that bed sorting and grain size range distribution greatly affect sediment transport. The site with the lowest mobility (S3) is also the site with the poorest bed sorting (Table 1). Previous studies indicate that a low relative grain size can increase the critical threshold for sediment mobilization (Mao et al., 2008; Gob et al., 2010; Parker et al., 2011). Our work shows that it may also affect bedload transport by limiting the travel distance. This effect may be seen as the result of higher critical conditions: (i) for sediment entrainment, delaying sediment departure; (ii) for sediment transport itself, with coarse grains that stand in the way or increase flow resistance, then reducing sediment step length.

The dominant influence of relative grain size on bedload tracer distances may have implications on the type of bedload mobility occurring in Morvan rivers. Indeed, the hidden / exposure effect due to relative grain size is likely to foster selective mobility and even an equal mobility in the stream beds where sediment motion is the most determined by relative grain size (Robert, 1993, 2003; Wohl, 2014). Equal mobility due to the presence of large particles on the bed has been notably underlined by Klösch and Habersack (2018) on the Puerto Rican Mameyes river (data from Phillips et al., 2013), which has a similar morphology to the Morvan rivers. The low bedload tracer distances on the S3 site could then come from the quasi absence of movement of coarse particles that hide the smaller ones and foster the formation of pebble clusters and other imbricated structures. The question of the current competence of the river and its ability to entrain these very coarse grains is therefore essential for the general mobility of all gravel fractions.

Conditions around equal mobility are all the more likely to occur when there is a deficit of the medium grain size fraction and a more or less well-formed armored layer (Parker and Klingeman, 1982). On the S3 Cure site, one may notice a highly stable interlocked configuration around large grains but not really the mobile armor in the surface layer that is often associated with equal mobility (Parker and Klingeman, 1982). In fact, the bed of the Cure on the S3 reach corresponds to a static armor (Sutherland, 1987; Parker and Sutherland, 1990). This is also why conditions of equal mobility are partial on the S3 Cure site: critical conditions for erosion and transport, and entrainment resistance are heightened for medium and small grain size fractions (low relative grain size, and potential imbrication) but they seem to remain very high for coarse, apparently immobile, cobbles and boulders.

Big particles are also present on the S7 Yonne river site but they lay among a considerable amount of medium grain size fractions (see sorting index in Table 1). This lower heterogeneity of the substrate and the lower relative grain size explain the differences of mean distances regarding S3, especially with stream impulse values and slope that are comparable and quite close on both sites. In the S7 morpho-sedimentary configuration, the sheltering effect of coarse cobbles and boulders also exists but influences the displacement of smaller particles to a lesser degree.

The dominant influence of the relative grain size on bedload distances underlines the influence of micro bed topography, especially in plane-bed rivers with heterogeneous grain size distribution. Indeed, in the absence of medium or large-scale bedforms consuming the river's' energy (meanders, alluvial bars, step-pool or riffle-pool sequences, etc.) (Petit et al., 2005), the role of the surrounding particles in the entrainment resistance of a given particle (sheltering / protrusion effect) is all the more important. This also invites us to examine more deeply the influence on bedload distances of small-scale characteristics other than relative grain size, such as imbrication degree, micro-scale bed forms (e.g. pebble clusters) and grain scale flow resistance (Robert, 1990, 2003; Lamb et al., 2017) in the context of plane-bed morphology.

5.4. The complex influence of the slope on bedload mean distances

The bed slope is the second most significant parameter influencing mean bedload distance according to our multivariate analysis. The first reason is of course that slope conditions the energy of the river. The second reason is less obvious, it is because slope may increase flow resistance by favoring a low relative flow depth (Bathurst, 2002; Lamb et al., 2008; Parker et al., 2011; Lamb et al., 2017). This leads to a decrease of the transport rate and/or an increase in critical conditions (Mizuyama, 1977; Shvidchenko and Pender, 2000; Mao et al., 2008; Chiari et al., 2010; Parker et al., 2011; Prancevic and Lamb, 2015; Bunte et al., 2013; Lamb et al., 2017). A low relative flow depth may also lower transport activity by reducing the intensity of turbulent fluctuations (Sumer et al., 2003; Lamb et al., 2017). All these elements are partly supported by our study in which bedload distances appear positively correlated to relative flow depth (Fig. 7C). However, from our multivariate analysis it emerged the relative flow depth was an insignificant explanatory variable despite its evident link with the slope.

For the S5 and S3 study sites, slope appears to be negatively correlated to bedload distances. S3 has the highest bed slope (with S7) but the shortest mean distance (for comparable SI) (Tables 1 and 3; Fig. 6). On the other hand, S5 distances are in the high range of intermediary distances while having the lowest slope (Tables 1 and 3; Fig. 6). Several studies already emphasized the positive relationship between slope and critical shear stress (Mizuyama, 1977; Mueller et al., 2005; Lamb et al., 2008; Gob et al., 2010; Parker et al., 2011). The negative correlation between slope and bedload distances we observe on several of our sites is therefore not totally unexpected. Slope may lower bedload distances when its effect is dominated by an increased flow resistance and energy loss. As for relative grain size, these “negative effects” of

slope may diminish bedload distances in two ways: they may heighten critical conditions for sediment entrainment and then delay their incipient motion for a flood event or reduce the frequency of mobilization; they may also lead the mobilized particles to settle faster and then reduce the displacement length.

Among the three sites with the steepest slopes (S3, S7, S8), two (S7 and S8) have logically the longest mean distances (for a comparable SI) (Tables 1 and 3; Fig. 6). They also have a higher relative depth and relative grain size compared to S3. This is also true for the three remaining sites (S2, S5 and S6) with a lower slope and lower intermediary mean distances. In line with S2, S6, S7 and S8 data, travel distance tends to increase with channel slope. These observations suggest that slope acts positively on bedload transport as long as relative depth and relative grain size remain above a certain threshold (in our case ≈2.5 and 0.50 respectively).

The S5 Chalaux site differs slightly from this trend: globally it presents comparable or higher distances than the S2 Cure site and the S6 Yonne site, with the highest relative depth and relative grain size, but with the lowest slope (Tables 1 and 3; Fig. 6). It is also the site with the lowest w/d ratio, even if the direct influence of this parameter on bedload transport was not recognized as significant. These elements imply that the impact of slope on transport may be a function of its combination with other parameters such as flow depth, determined by discharge, flow velocity and river geometry, grain size distribution of the river bed, etc. It may also suggest that if slope may heighten critical conditions for sediment entrainment (Mizuyama, 1977; Lamb et al., 2008; Gob et al., 2010; Parker et al., 2011), in some situations (S7 and S8), it may increase sediment displacement length once particles are put in motion. The seemingly ambivalent role of slope on Morvan rivers calls to mind the observation of Prancevic and Lamb (2015) of the absence of a universal trend in the relationship between critical dimensionless shear stress and channel slope.

5.5. Validity of the model equation and methodological choices

The different results presented in this paper have been, for the most part, statistically valid and the model equation (Eq. (4)) obtained from the multiple linear regressions have been convincingly validated by the independent data set of the Aisne river. The margin of error associated with bedload displacement (0.6 to 1 m, due to the precision of the RFID Antenna and the precision of our methodology to survey the tagged particles) may be considered as quite low. Indeed, mean travel distance per inter-survey period is 16.3 m (immobile tracers included). The error associated with the marked particle location represents therefore only 4 to 6% of the distance travelled.

Several choices that have been made in this paper could have led to uncertainties that may call into question our results and, therefore, require further discussion.

The first of these choices concerns the threshold for sediment incipient motion. Unfortunately, it was not possible to determine this precisely from our RFID surveys. Yet the critical discharge is a key parameter for the calculation of stream impulse or excess stream power. Our choice to consider a threshold that equals $0.7^{*}Q_{bf}$ is therefore a strong assumption that has been widely discussed in the methods section. In the end, our results show that our choice was probably quite accurate, especially since Eq. (4) has provided very good estimations of travel distance for the independent data of the Aisne river, for which the incipient motion threshold has been determined empirically on the field. Having said that, further investigations on the exact critical discharge would be worthwhile.

The second of our methodological choices that could have led to a certain level of uncertainty concerns the size of the largest particles tagged. Indeed, because of our tagging protocol, the coarsest particles of the riverbed (>175 mm) were not tagged. This may have induced an underestimation of the maximum competence of the river. However, we think that these large cobbles and blocks that have not been marked are in fact immobile. Firstly, the largest particles we tagged did not moved or barely moved (Table 3 and Fig. 4). Secondly, several indications such as moss, black biofilm, stable imbrication, etc. show that the largest cobbles and the boulders present in the bed should not be considered as bedload under the current hydrological conditions.

6. Conclusions

The bedload transport of Morvan rivers is complex and depends on a range of parameters. The multi-peak characteristic of our surveys requires the integration of every discharge over the critical threshold, in terms of intensity and duration, and not only the highest peak, in order to evaluate the hydrological influence on bedload travel distances. The time integrated energy parameter we use – stream impulse – enables us to give more meaning to our data. However, it is not sufficient to fully understand the recorded differences of bedload displacements as the dispersion of tracer distances draws three distinct relationships. Also, when plotted with a classical energy indicator (excess specific stream power), bedload displacements cover a wide range of values obtained from other studies on different channel morphological types (plane-bed, riffle-pool, step-pool). This variability of distance values leads us to investigate the influence of more specific morphological and hydraulic parameters (and the role of their own variability) on bedload transport in a plane-bed context. The stream impulse and the other four hydro-morphometric parameters that we tested (relative grain size, relative flow depth, slope, w/d ratio) bring us useful information to highlight what controls bedload transport on Morvan rivers. The multiple regression analysis indicates that the relative grain size, the slope and the stream impulse are, in order of significance, the most important parameters influencing bedload distances.

Relative grain size, the first controlling factor on bedload mean distance on Morvan rivers, emphasizes the importance of microtopography and grain size distribution range in plane-bed rivers. Substrate arrangement and very coarse particles compose various grain/micro to medium scale features. These are probably even more important to consider in this plane-bed channel morphology as they represent the main constraints to particle entrainment (hiding effect, imbrication, stable sedimentary structures) and the main sources of flow resistance (immobile cobbles and boulders, transverse ribs, clusters).

The role of the slope has already been studied in relation to critical conditions for incipient motion. Our study shows that it significantly affects direct bedload distances. The way in which bed slope has an influence is ambiguous though, and seems to depend on other hydro-morphometric factors: it notably appears to act in favor of bedload travel distances when the coarsest particles are largely submerged ($d/D_{84} > 2.5$ at least). Nonetheless, the multiple regression suggests that slope impacts bedload distances more significantly in other ways.

The single model equation we obtained to predict mean bedload distance (Eq. (4)), combining stream impulse (SI), relative grain size and bed slope, functions pretty well with our own data and with data from the Aisne river. However, it is wise to pursue these validation tests further, with other data that are equivalent to ours (data collection method, geomorphological settings). If validity is confirmed, tests with other morphological types of fluvial systems and in different morpho-climatic contexts will be needed to determine the application range of the model.

Acknowledgments

The authors would like to thank Matthieu Moës and the Agence de l'Eau Seine-Normandie (public water agency), for financing the research work leading to this paper. We are also very grateful to Jean-René Malavoi and Electricité de France (EDF) as well as the PIREN Seine for the financial support they provided for the purchase of research equipment and for fieldwork missions. We extend our sincere appreciation to Jonathan Touche for his help on the field and Natasha Shields for her assistance in translating. Finally, we would like to thank F. Comiti and the

anonymous reviewer for their thoughtful comments that enabled the quality of the original paper to be greatly improved.

References

Andrews, E.D., Nankervis, J.M., 1995. Effective discharge and the design of channel maintenance flows for gravel-bed rivers. Geophys. Monog. Ser. 89, 151–164.

Arnaud, F., Piégay, H., Vaudor, L., Bultingaire, L., Fantino, G., 2015. Technical specifications of low-frequency radio identification bedload tracking from field experiments: differences in antennas, tags and operators. Geomorphology 238, 37–46.

Arnaud, F., Piégay, H., Béal, D., Collery, P., Vaudor, L., Rollet, A.J., 2017. Monitoring gravel augmentation in a large regulated river and implications for process-based restoration. Earth Surf. Process. Landf. 42 (13), 2147–2166.

Assani, A.A., Petit, F., 2004. Impact of hydroelectric power releases on the morphology and sedimentology of the bed of the Warche river (Belgium). Earth Surf. Process. Landf. 29, 133–143.

Bagnold, R.A., 1980. An empirical correlation of bedload transport rates in flumes and natural rivers. Proc. R. Soc. Lond. A 372, 453–473.

Bathurst, J.C., 2002. At-a-site variation and minimum flow resistance for mountain rivers. J. Hydrol. 269, 11–26.

Belliard, J., Albert, M.B., Gob, F., Sauquet, E., Catalogne, C., Zahm, A., 2009. Caractérisation des altérations physiques et de leurs conséquences écologiques des rivières du bassin Seine-Normandie. Phase I: cas des cours d'eau de la Craie. Seine Normandie (AESN)/Cemagref, Accord-cadre Agence de l'Eau (85 p.).

Bradley, N., Tucker, G.E., 2012. Measuring gravel transport and dispersion in a mountain river using passive radio tracers. Earth Surf. Process. Landf. 37, 1034–1045.

Bravard, J.P., Petit, F., 1997. Les Cours d'eau, Dynamique du Système Fluvial. Armand Colin, Paris (222 pp).

Bright, C.J., 2014. Development of an RFID Approach to Monitoring Bedload Sediment Transport and a Field Case Study. Ph.D thesis. University of Waterloo (255 pp).

Bunte, K., Abt, S.R., Swingle, K.W., Cenderelli, D.A., Schneider, J.M., 2013. Critical shields values in coarse bedded steep streams. Water Resour. Res. 49, 7427–7447.

Chapuis, M., Bright, C.J., Hufnagel, J., MacVicar, B., 2014. Detection ranges and uncertainty of passive Radio Frequency Identification (RFID) transponders for sediment tracking in gravel rivers and coastal environments. Earth Surf. Process. Landf. 39, 2109–2120.

Chiari, M., Friedl, K., Rickenmann, D., 2010. A one-dimensional bedload transport model for steep slopes. J. Hydraul. Res. 48 (2), 152–160.

Church, M., Hassan, M.A., 1992. Size and distance of travel of unconstrained clasts on a streambed. Water Resour. Res. 28, 299–303.

Dell'Agnese, A., Brardinoni, F., Toro, M., Mao, L., Engel, M., Comiti, F., 2015. Bedload transport in a formerly glaciated mountain catchment constrained by particle tracking. Earth Surf. Dyn. 3, 527–542.

Dépret, T., Gautier, E., Hooke, J., Grancher, D., Virmoux, V., Brunstein, D., 2017. Causes of planform stability of a low-energy meandering gravel-bed river (Cher River, France). Geomorphology 285, 58–81.

Ferguson, R., Hoey, T., 2002. Long-term slowdown of river tracer pebbles: generic models and implications for interpreting short-term tracer studies. Water Resour. Res. 38 (8, 1142) (17-1-17-11).

Ferguson, R., Wathen, S., 1998. Tracer-pebble movement along a concave river profile: virtual velocity in relation to grain size and shear stress. Water Resour. Res. 34, 2031–2038.

Ferguson, R.I., Bloomer, D.J., Hoey, T.B., Werritty, A., 2002. Mobility of river tracer pebbles over different timescales. Water Resour. Res. 38 (5, 1045) (3-1-3-8).

Gilet, L., Gob, F., Virmoux, C., Touche, J., Harrache, S., Gautier, E., Moës, M., Thommeret, N., Jacob-Rousseau, N., 2018. Suivi de l'évolution morphologique et sédimentaire de l'Yonne suite à la première phase du démantèlement du barrage de Pierre Glissotte (Massif du Morvan, France). Géomor. Relief Proc. Environ. 24 (1), 7–29.

Gintz, D., Hassan, M.A., Schmidt, K.H., 1996. Frequency and magnitude of bedload transport in a mountain river. Earth Surf. Process. Landf. 21, 433–445.

Gob, F., Bravard, J.P., Petit, F., 2010. The influence of sediment size, relative grain size and channel slope on initiation of sediment motion in boulder bed rivers. A lichenometric study. Earth Surf. Process. Landf. 35, 1535–1547.

Haschenburger, J.K., 2011. The rate of fluvial gravel dispersion. Geophys. Res. Lett. 38 (L24403).

Haschenburger, J.K., 2013. Tracing river gravels: insights into dispersion from a long-term field experiment. Geomorphology 200, 121–131.

Haschenburger, J.K., Church, M., 1998. Bed material transport estimated from the virtual velocity of sediment. Earth Surf. Process. Landf. 23, 791–808.

Hassan, M., Bradley, D.N., 2017. Geomorphic controls on tracer particle dispersion in gravel bed rivers. In: Tsutsumi, D., Laronne, J.B. (Eds.), Gravel-Bed Rivers. Processes and Disasters, Wiley-Blackwell, UK, pp. 439–466.

Hassan, M.A., Church, M., 1992. The movement of individual grains on the streambed. In: Billi, P., Hey, R.D., Thorne, C.R., Tacconi, P. (Eds.), Dynamics of Gravel-Bed Rivers. Wiley, New-York, pp. 159–175.

Hassan, M.A., Church, M., Schick, A.P., 1991. Distance of movement of coarse particles in gravel bed streams. Water Resour. Res. 27, 503–511.

Hassan, M.A., Church, M., Ashworth, P.J., 1992. Virtual rate and mean distance of travel of individual clasts in gravel-bed channels. Earth Surf. Process. Landf. 17, 617–627.

Houbrechts, G., Hallot, E., Gob, F., Mols, J., Defechereux, O., Petit, F., 2006. Frequency and extent of bedload transport in rivers of the Ardenne. Géog. Phys. Quatern. 60 (3), 247–258.

Houbrechts, G., Campenhout, J.V., Levecq, Y., Hallot, E., Peeters, A., Petit, F., 2012. Comparison of methods for quantifying active layer dynamics and bedload discharge in armoured gravel-bed rivers. Earth Surf. Process. Landf. 37, 1501–1517.

Houbrechts, G., Levecq, Y., Peeters, A., Hallot, E., Campenhout, J.V., Denis, A.C., Petit, F., 2015. Evaluation of long-term bedload virtual velocity in gravel-bed rivers (Ardenne, Belgium). Geomorphology 251, 6–19.

Jaeggi, M.N.R., 1987. Interaction of Bed Load Transport With Bars. Thorne, C.R, Bathurst.

Klösch, M., Habersack, H., 2018. Deriving formulas for an unsteady virtual velocity of bedload tracers. Earth Surf. Process. Landf. 43, 1529–1541.

Lamarre, H., Roy, A.G., 2008. The role of morphology on the displacement of particles in a step–pool river system. Geomorphology 99, 270–279.

Lamarre, H., Roy, A.G., MacVicar, B., 2005. Using PIT tags to investigate sediment transport in gravel-bed rivers. J. Sediment. Res. 75 (4), 736–741.

Lamb, M.P., Dietrich, W.E., Venditti, J.G., 2008. Is the critical Shields stress for incipient sediment motion dependent on channel-bed slope? J. Geophys. Res. Earth Surf. 113 (F02008).

Lamb, M.P., Brun, F., Fuller, B.M., 2017. Direct measurements of lift and drag on shallowly submerged cobbles in steep streams: implications for flow resistance and sediment transport. Water Resour. Res. 53 (9), 7607–7629.

Laronne, J.B., Outhet, D.N., Duckman, J.L., 1992. Determining event bedload volume for evaluation of potential degradation sites due to gravel extraction, N.S.W., Australia. Erosion and Sediment Transport Monitoring Programmes in River Basins (Proceedings of the Oslo Symposium, August 1992), IAHS Publications 210. IAHS Press, Wallingford, pp. 87–94.

Lejot, J., 2008. Suivi des formes fluviales par télédétection à très haute résolution. Application aux Programmes de Restauration de la Basse Vallée de l'Ain et du Haut-Rhône (Chautagne). Université Lumière Lyon 2 Thèse de doctorat. (257p).

Lenzi, M.A., 2004. Displacement and transport of marked pebbles, cobbles and boulders during floods in a steep mountain stream. Hydrol. Process. 18, 1899–1914.

Liébault, F., Clément, P., 2007. La mobilité de la charge de fond des rivières torrentielles méditerranéennes. Géog. Phys. Quatern. 61 (1), 7–20.

Liébault, F., Laronne, J.B., 2008. Evaluation of bedload yield in gravel-bed rivers using scour chains and painted tracers: the case of the Esconavette Torrent (southern French Prealps). Geodin. Acta 21, 23–34.

Liébault, F., Bellot, H., Chapuis, M., Klotz, S., Deschâtres, M., 2012. Bedload tracing in a high-sediment-load mountain stream. Earth Surf. Process. Landf. 37, 385–399.

Madej, M.A., Ozaki, V., 1996. Channel response to sediment wave propagation and movement, Redwood Creek, California, USA. Earth Surf. Process. Landf. 21, 911–927.

Mao, L., Uyttendaele, G.A., Iroumé, A., Lenzi, M.A., 2008. Field based analysis of sediment entrainment in two high gradient streams located in Alpine and Andine environments. Geomorphology 93, 368–383.

Mao, L., Picco, P., Lenzi, M.A., Surian, N., 2017a. Bed material transport estimate in large gravel-bed rivers using the virtual velocity approach. Earth Surf. Process. Landf. 42, 595–611.

Mao, L., Dell'Agnese, A., Comiti, F., 2017b. Sediment motion and velocity in a glacier-fed stream. Geomorphology 291, 69–79.

Métivier, F., Lajeunesse, E., Devauchelle, O., 2017. Laboratory rivers: Lacey's law, threshold theory, and channel stability. Earth Surf. Dyn. 5, 187–198.

Milan, D.J., 2013. Virtual velocity of tracers in a gravel-bed river using size-based competence duration. Geomorphology 198, 107–114.

Mizuyama, T., 1977. Bedload Transport in Steep Channels. Ph.D thesis. University of Kyoto (123 pp).

Moog, D.B., Whiting, P.J., 1998. Annual hysteresis in bed load rating curves. Water Resour. Res. 34 (9), 2393–2399.

Mueller, E.R., Pitlick, J., Nelson, J.M., 2005. Variation in the reference Shields stress for bed load transport in gravel-bed streams and rivers. Water Resour. Res. 41 (4), 1–10.

Olinde, L., Johnson, J.P.L., 2015. Using RFID and accelerometer-embedded tracers to measure probabilities of bed load transport, step lengths, and rest times in a mountain stream. Water Resour. Res. 51, 7572–7589.

Papangelakis, E., 2013. The Effects of Channel Morphology on the Mobility and Dispersion of Sediment in a Small Gravel-Bed Stream. University of Toronto, Master thesis (93 pp).

Papangelakis, E., Hassan, M., 2016. The role of channel morphology on the mobility and dispersion of bed sediment in a small gravel-bed stream. Earth Surf. Process. Landf. 41, 2191–2206.

Parker, G., Klingeman, P.C., 1982. On why gravel-beds streams are paved. Water Resour. Res. 18, 1409–1423.

Parker, G., Sutherland, A.J., 1990. Fluvial armour. J. Hydraul. Res. 28, 529–544.

Parker, C., Clifford, N.J., Thorne, C.R., 2011. Understanding the influence of slope on the threshold of coarse grain motion: revisiting critical stream power. Geomorphology 126, 51–65.

Petit, F., Gob, F., Houbrechts, G., Assani, A.A., 2005. Critical specific stream power in gravel-bed rivers. Geomorphology 69 (1–4), 92–101.

Pfeiffer, A.M., Finnegan, N.J., Willenbring, J.K., 2017. Sediment supply controls equilibrium channel geometry in gravel rivers. PNAS 114 (13), 3346–3351.

Phillips, J.D., 2015. Hydrologic and geomorphic flow thresholds in the Lower Brazos River, Texas, USA. Hydrol. Sci. J. 60 (9), 1631–1647.

Phillips, C.B., Jerolmack, D.J., 2014. Dynamics and mechanics of bed-load tracer particles. Earth Surf. Dyn. 2, 513–530.

Phillips, C.B., Martin, Raleigh, L., Jerolmack, D.J., 2013. Impulse framework for unsteady flows reveals superdiffusive bed load transport. Geophys. Res. Lett. 40, 1328–1333.

Piégay, H., Arnaud, F., Cassel, M., Dépret, T., Alber, A., Michel, K., Rollet, A.J., Vaudor, L., 2016. Suivi par RFID de la mobilité des galets: retour sur 10 ans d'expérience en grandes rivières. Bulletin de la Société Géographique de Liège 67, 77–91.

Pitlick, J., Cress, R., 2000. Longitudinal trends in channel characteristics of the Colorado River and implications for food-web dynamics. Final Report to the Recovery Program for the Endangered Fishes of the Upper Colorado River, Project Number 48, Department of Geography. University of, Colorado (52 pp).

Prancevic, J., Lamb, M.P., 2015. Unraveling bed slope from relative roughness in initial sediment motion. J. Geophys. Res. Earth Surf. 120 (3), 474–489.
Pyrce, R.S., Ashmore, P.E., 2003a. The relation between particle path length distributions and channel morphology in gravel-bed streams: a synthesis. Geomorphology 56, 167–187.
Pyrce, R.S., Ashmore, P.E., 2003b. Particle path length distributions in meandering gravel-bed streams: results from physical models. Earth Surf. Process. Landf. 28 (9), 951–966.
Pyrce, R.S., Ashmore, P.E., 2005. Bedload path length and point bar development in gravel-bed river models. Sedimentology 52, 839–857.
Robert, A., 1990. Boundary roughness in coarse-grained channels. Prog. Phys. Geogr. Earth Environ. 14, 42–70.
Robert, A., 1993. Bed configuration and microscale processes in alluvial channels. Prog. Phys. Geogr. 17 (2), 123–136.
Robert, 2003. A. River Processes. Hodder Education, London (214 pp).
Rollet, A.J., Macvicar, B., Piégay, H., Roy, A., 2008. Utilisation de transpondeurs passifs pour l'estimation du transport sédimentaire: premiers retours d'expérience. La Houille Blanche - Revue internationale de l'eau, EDP Sciences 2008.
Scheingross, J.S., Winchell, E.W., Lamb, M.P., Dietrich, W.E., 2013. Influence of bed patchiness, slope, grain hiding, and form drag on gravel mobilization in very steep streams. J. Geophys. Res. Earth Surf. 118, 982–1001.
Schneider, J., Turowski, J., Rickenmann, D., Hegglin, R., Arrigo, S., Mao, L., Kirchner, J., 2014. Scaling relationships between bed load volumes, transport distances, and stream power in steep mountain channels. J. Geophys. Res. Earth Surf. 119 (3), 533–549.
Shvidchenko, A.B., Pender, G., 2000. Flume study of the effect of relative depth on the incipient motion of coarse uniform sediments. Water Resour. Res. 36 (2), 619–628.
Sumer, B.M., Chua, L.H.C., Cheng, N.S., Fredsoe, J., 2003. Influence of turbulence on bed load sediment transport. J. Hydraul. Eng. 129, 585–595.
Sutherland, A.J., 1987. Static armor layers by selective erosion. In: Thorne, C.R., Bathurst, J.C., Hey, R.D. (Eds.), Sediment Transport in Gravel-Bed Rivers. Wiley, Chichester, pp. 243–267.
Sutherland, D.G., Hansler Ball, M., Hilton, S.J., Lisle, T.E., 2002. Evolution of a landslide induced sediment wave in the Navarro River, California. Geol. Soc. Am. Bull. 114 (8), 1036–1048.
Wilcock, P.R., 1997. Entrainment, displacement, and transport of tracer gravels. Earth Surf. Process. Landf. 22, 1125–1138.
Wohl, E., 2014. Rivers in the Landscape. Wiley-Blackwell, UK (330 pp).
Wolman, M.G., 1954. A method of sampling coarse bed material. Am. Geophys. Union Trans. 35, 951–956.